1-2012

Remodeling the Isoprenoid Pathway in Tobacco by Expressing the Cytoplasmic Mevalonate Pathway in Chloroplasts

Shashi Kumar

Frederick M. Hahn

Edward Baidoo

Talwinder S. Kahlon

Delilah F. Wood

Recommended Citation

Kumar, S., Hahn, F. M., Baidoo, E., Kahlon, T. S., & Wood, D. F. (2012). Remodeling the Isoprenoid Pathway in Tobacco by Expressing the Cytoplasmic Mevalonate Pathway in Chloroplasts. *Metabolic Engineering, 14* (1), 19-28. http://dx.doi.org/10.1016/j.ymben.2011.11.005

At the time of publication, author Henry Daniell was affiliated with the University of Central Florida. Currently, he is a faculty member at the School of Dental Medicine at the University of Pennsylvania.

Remodeling the Isoprenoid Pathway in Tobacco by Expressing the Cytoplasmic Mevalonate Pathway in Chloroplasts

Abstract

Metabolic engineering to enhance production of isoprenoid metabolites for industrial and medical purposes is an important goal. The substrate for isoprenoid synthesis in plants is produced by the mevalonate pathway (MEV) in the cytosol and by the 2-C-methyl-D-erythritol 4-phosphate (MEP) pathway in plastids. A multi-gene approach was employed to insert the entire cytosolic MEV pathway into the tobacco chloroplast genome. Molecular analysis confirmed the site-specific insertion of seven transgenes and homoplasmy. Functionality was demonstrated by unimpeded growth on fosmidomycin, which specifically inhibits the MEP pathway. Transplastomic plants containing the MEV pathway genes accumulated higher levels of mevalonate, carotenoids, squalene, sterols, and triacyglycerols than control plants. This is the first time an entire eukaryotic pathway with six enzymes has been transplastomically expressed in plants. Thus, we have developed an important tool to redirect metabolic fluxes in the isoprenoid biosynthesis pathway and a viable multigene strategy for engineering metabolism in plants.

Keywords

Plant metabolic engineering, Mevalonate pathway, Methylerythritol phosphate pathway, Chloroplast engineering, Tobacco, Isoprenoid biosynthesis

Disciplines

Dentistry

Comments

At the time of publication, author Henry Daniell was affiliated with the University of Central Florida. Currently, he is a faculty member at the School of Dental Medicine at the University of Pennsylvania.

HHS Public Access

Author manuscript

Metab Eng. Author manuscript; available in PMC 2018 January 14.

Published in final edited form as:

Metab Eng. 2012 January ; 14(1): 19–28. doi:10.1016/j.ymben.2011.11.005.

Remodeling the isoprenoid pathway in tobacco by expressing the cytoplasmic mevalonate pathway in chloroplasts

Shashi Kumar[a,b,1], **Frederick M. Hahn**[a], **Edward Baidoo**[c], **Talwinder S. Kahlon**[a], **Delilah F. Wood**[a], **Colleen M. McMahan**[a], **Katrina Cornish**[b,2], **Jay D. Keasling**[c], **Henry Daniell**[d], and **Maureen C. Whalen**[a,*]

[a]Western Regional Research Center, Agricultural Research Service, United States Department of Agriculture, Albany, CA, United States

[b]Yulex Corporation, Maricopa, AZ, United States

[c]Joint BioEnergy Institute, Lawrence Berkeley National Laboratory, Emeryville, CA, United States

[d]Department of Molecular Biology & Microbiology, College of Medicine, University of Central Florida, Orlando, FL, United States

Abstract

Metabolic engineering to enhance production of isoprenoid metabolites for industrial and medical purposes is an important goal. The substrate for isoprenoid synthesis in plants is produced by the mevalonate pathway (MEV) in the cytosol and by the 2-C-methyl-D-erythritol 4-phosphate (MEP) pathway in plastids. A multi-gene approach was employed to insert the entire cytosolic MEV pathway into the tobacco chloroplast genome. Molecular analysis confirmed the site-specific insertion of seven transgenes and homoplasmy. Functionality was demonstrated by unimpeded growth on fosmidomycin, which specifically inhibits the MEP pathway. Transplastomic plants containing the MEV pathway genes accumulated higher levels of mevalonate, carotenoids, squalene, sterols, and triacyglycerols than control plants. This is the first time an entire eukaryotic pathway with six enzymes has been transplastomically expressed in plants. Thus, we have developed an important tool to redirect metabolic fluxes in the isoprenoid biosynthesis pathway and a viable multigene strategy for engineering metabolism in plants.

Keywords

Plant metabolic engineering; Mevalonate pathway; Methylerythritol phosphate pathway; Chloroplast engineering; Tobacco; Isoprenoid biosynthesis

*Corresponding author. Fax: +1 510 559 5634. maureen.whalen@ars.usda.gov (M.C. Whalen).

Present address: International Center of Genetic Engineering and Biotechnology, Aruna Asaf Ali Marg, New Delhi, India.

Present address: Department of Horticulture and Crop Science, Department of Food, Agricultural and Biological Engineering, The Ohio State University, Ohio Agricultural Research and Development Center, Wooster, Ohio, United States.

Disclosure statement

Jay D. Keasling has a financial interest in Amyris Biotechnologies, Inc., a company that produces isoprenoid-based chemicals and fuels.

1. Introduction

Strategies to engineer secondary metabolism in plants have evolved away from step-by-step schemes to more holistic designs, in which expression of multiple enzymes are altered and the impact of the perturbation on the entire system is studied (Capell and Christou, 2004). These strategies include manipulation of existing pathways in either a positive or a negative manner and introduction of completely novel pathways. Metabolic engineering of plants to enhance production of a diversity of isoprenoids remains an important goal (Kirby and Keasling, 2009). Isoprenoid biosynthetic pathways are responsible for the formation of the most chemically diverse family of metabolites found in nature, including sterols (C30), carotenoids (C40), dolichols (C40–50), ubiquinones (C30–50), and natural rubber (C2,000–300,000). Phytohormones are also derived from the pathway, including abscisic acid (C15), gibberellins (C20), and brassinosteroids (C30). Many plant isoprenoids have pharmaceutical importance, but more progress has been made in engineering microbes to produce bioactive plant isoprenoids, such as the anti-malarial compound artemisinin (Kirby and Keasling, 2009), than in plants.

Biosynthesis of isopentenyl diphosphate (IPP) and dimethylallyl diphosphate (DMAPP), the two essential 5-carbon isoprenoid building-blocks, occurs by two distinct routes in plants in the cytosol and in plastids (Lichthentaler, 2007). In the cytosol, IPP and DMAPP are assembled from three molecules of acetyl Co-A by the mevalonate (MEV) pathway. In plastids an independent pathway, called the 2-C-methyl-D-erythritol 4-phosphate (MEP) pathway, makes IPP and DMAPP from pyruvate and glyceraldehyde 3-phosphate. The MEV pathway provides precursors for the synthesis of sterols, brassinosteroids, ubiquinone and sesquiterpenes, whereas the MEP pathway is associated with the synthesis of isoprene, monoterpenes, diterpenes, carotenoids, abscisic acid, and the side chains of chlorophylls, tocopherols, and plastoquinone. In plants, thousands of isoprenoids are synthesized from IPP and DMAPP by diverse pathways downstream of the MEP and MEV pathways.

Exchange of metabolites takes place between the cytosol and plastids (Bick and Lange, 2003; Laule et al., 2003) in the synthesis of different isoprenoid metabolites (Dudareva et al., 2005; Gerber et al., 2009; Kasahara et al., 2002; Nagata et al., 2002; Steliopoulos et al., 2002). The extent of the exchange is an important question to cellular engineering strategies. Interestingly, inhibiting the cytosolic MEV pathway ultimately resulted in seedling death (Bach and Lichtenthaler, 1983), despite the full functioning of the MEP pathway, as evidenced by normal levels of chlorophylls, carotenoids, and plastoquinone in the chloroplasts. Thus, over time in that case and in the case of male gametophytes (Suzuki et al., 2009) the MEP pathway was unable to fully and efficiently compensate for the loss in function of the MEV pathway. Additionally, chloroplast development and overall plant growth were adversely affected in a study using Arabidopsis *cla*1-1 mutants that do not express the enzyme for the first step in the MEP pathway (Mandel et al., 1996) even though metabolites flow from the MEV pathway to the plastid (Nagata et al., 2002). Thus, the MEV pathway did not fully compensate for the genetic inhibition of the MEP pathway. It is clear that the experimental system, for example cells in liquid culture vs. whole plants or inhibition of biosynthetic pathways by mutation or chemical inhibitors, would dramatically influence results (Hammerlin and Bach, 1998). Isolated chloroplasts and chloroplast

membranes were shown to export the precursor IPP (C5) and geranyl diphosphate (GPP; C10), and less efficiently, farnesyl diphosphate (FPP; C15) and dimethylallyl diphosphate (DMAPP; C5), whereas geranylgeranyl diphosphate (GGPP; C20) and mevalonate were not exported (Bick and Lange, 2003). Some of these results conflict with those derived from other experimental systems (e.g., Gerber et al., 2009; Kasahara et al., 2002). If chloroplast engineering is to be used as a strategy to produce isoprenoid substrates that are available to cytosolic pathways, the level of exchange between the two compartments remains an important question.

Genes that express the enzymes of the MEV, MEP, and downstream pathways have been manipulated to enhance carbon flow into specific downstream products. The body of literature on these genetic manipulations suggests that, in most cases, synthesis of the upstream isoprenoid precursors IPP and DMAPP should be maximized to boost production of downstream metabolites. The rate-limiting step in the MEV pathway, 3-hydroxy-3methyl-glutaryl-coenzyme A reductase (HMGR) has been the target of genetic manipulations in several studies. Over-expression of heterologous HMGR resulted in increased levels of total sterols in tomato (Enfissi et al., 2005) and tobacco (Chappell et al., 1991; Harker et al., 2003; Schaller et al., 1995). Many other isoprenoid products have been successfully enhanced, including monoterpenes and sesquiterpenes (Davidovich-Rikanati et al., 2007, 2008). In a noteworthy study, coupled overexpression of FPP synthase (FPPS) with patchoulol synthase (PTS) increased levels of the terpene patchoulol by two- to five-fold (Wu et al., 2006). Moreover, adding the unregulated HMGR gene further enhanced production of patchoulol by an additional two- to six-fold. Production of the biosynthetic enzymes at the appropriate time in development (Enfissi et al., 2005), along with targeting to subcellular compartments (Hasunuma et al., 2008a), plays an important role in optimizing the impact of genetic manipulations of isoprenoids in plants.

Another approach to enhance isoprenoid production is manipulation of isoprenoid pathways in chloroplasts. This has been successfully accomplished in two ways. The first way is by fusing plastid-targeting sequences to nuclear transgenes and the second way is to engineer the genome of chloroplasts. Wu et al. (2006) further increased levels of the desired metabolite, patchoulol, by targeting FPPS and PTS transgene products to the chloroplast. In tomato fruits, the content of carotenoids changed when 1-deoxy-D-xylulose-5-phosphate synthase (DXS) was targeted to chloroplasts (Enfissi et al., 2005). Engineering chloroplasts directly has been successful in enhancing isoprenoid products. Tobacco plants overexpressing the MEP pathway enzyme 1-deoxy-D-xylulose 5-phosphate reductoisomerase (DXR) gene from the chloroplast genome had elevated levels of chlorophyll a, carotenoids, and sterols (Hasunuma et al., 2008a). Two bacterial genes expressed in chloroplasts of tobacco produced high levels of the carotene derivative astaxanthin in leaves (Hasunuma et al., 2008b). Most remarkably, expression of the daffodil lycopene β-cyclase gene in tomato chloroplasts resulted in a 52% increase in total carotenoids, with β-carotene (provitamin A) levels approaching 1 mg/g dry weight in fruits (Apel and Bock, 2009). High-level production of foreign proteins via chloroplast transformation, up to 72% of the total leaf protein (Oey et al., 2009; Ruhlman et al., 2010), is one of the major benefits of this engineering strategy. To date, up to six genes have been inserted at once (Krichevsky et al., 2010) with multigene engineering made possible by

translation of polycistrons generated from a single promoter (Quesada-Vargas et al., 2005). Expression levels have been optimized with insertion at the trnI/trnA site in the chloroplast genome (Krichevsky et al., 2010). Importantly, from the point of view of minimizing environmental impact, expressing foreign proteins in the chloroplast results in transgene containment (Daniell, 2007; Maliga, 1993), because chloroplasts are usually not transmitted by pollen.

In the metabolic engineering study reported here, we employed a multi-gene approach to express an entire cytosolic pathway in chloroplasts. We engineered chloroplasts of tobacco with the six genes encoding the cytoplasmic MEV pathway to increase synthesis of isoprenoid metabolites, plus a selectable marker gene. We demonstrate increased levels of products normally associated with both the chloroplastidic and the cytosolic pathways, including mevalonate, carotenoids, sterols, and squalene, as well as triacyl-glycerides. This report is the first describing integration of six foreign eukaryotic genes encoding a cytoplasmic pathway into the chloroplast genome and demonstrates a viable multigene strategy for metabolic engineering in plants.

2. Materials and methods

2.1. Construction of tobacco chloroplast transformation vectors

The plasmid pFCO1 contains a synthetic operon comprising half of the genes encoding the mevalonate pathway (Hahn et al., 2001), including the yeast open reading frames (orfs) encoding phosphomevalonate kinase (PMK, ERG8), mevalonate kinase (MVK, ERG12), and mevalonate diphosphate decarboxylase (MDD, ERG19). Each gene was engineered to contain sequences for a ribosome binding site at the 5′-end and coding sequences for Gln-Glu-Glu-Phe at the 3′-end. A pLDCtV (Guda et al., 2000) derivative containing a 6-gene cluster comprising the complete mevalonate pathway was constructed. The three genes encoding acetoacetyl CoA thiolase (AACT, ERG10), HMGCoA synthase (HMGS, ERG13), and a C-terminal truncated HMGCoA reductase (HMGRt) were amplified from yeast genomic DNA, and inserted into pCR2.1-TOPO according to the manufacturer's instructions (Invitrogen). The three genes were then cloned from their pCR plasmids and inserted sequentially into pSMART (Lucigen) to create a 3-gene cluster, followed by insertion of the 3.9-kb insert from pFCO1 to create pSM-MEV6. Finally, the tobacco chloroplast transformation vector pUY-MEV6, containing the 6-gene cluster comprising the complete yeast mevalonate pathway, was created by inserting the 8.2-kb EagI fragment from pSM-MEV6 into the *Not*I site of pLDCtV. The plasmid pUY-MEV6.1 is a corrected version of pUY-MEV6, in which 36 nucleotides that were missing from the 3′-end of AACT were added back using a synthetic DNA fragment (BioBasics). Fig. S1 contains the entire sequence of pUY-MEV6.1.

2.2. Chloroplast transformation and selection

The leaves of *Nicotiana tabacum* cv. Petit Havana SR1 were transformed as described in Kumar and Daniell (2004) using S550d gold particles according to manufacturer's instructions (SeaShell Technology). The independently generated transplastomic lines were subjected to 4–6 rounds of regeneration on RMOP/spectinomycin. To functionally confirm

the presence of the genes, transplastomic and wildtype calli were grown on RMOP medium (Kumar and Daniell, 2004) containing fosmidomycin at 100 μM. Fosmidomycin is a specific inhibitor of DXR in the plastidial MEP pathway (Zeidler et al., 1998).

2.3. Confirmation of integration into chloroplast genome and expression of transgenes

2.3.1. Genomic PCR analysis—To test integration of gene cassettes into the chloroplast genome of tobacco, PCR was performed with primers that were targeted to the introduced *aad*A gene and native chloroplast genomic DNA. Primer aadA-midF, CGACATTGATCTGGCTATCTTGCTGACA, targets the internal region of the *aad*A gene, and primer 23S-Rev, ATTAC-TACGCCCTTCCTCGTCTCTGGG, targets the chloroplast genome in the 23S region adjacent to the insertion site (Fig. 1).

2.3.2. Genomic southern blot analysis—In addition, Southern blots were performed to analyze integration. Total genomic DNA (2 μg) was isolated using the DNeasy Plant Mini kit (Qiagen) according to vendor's instructions. Genomic DNA of transgenics and wildtype was digested with *Afl*III and *Pvu*II; that of the empty vector control was digested with *Afl*III, *Pvu*II, and *Xba*I. DNA blots were hybridized with a 0.8-kb P^{32}-labeled DNA probe amplified by the PCR using primers to internal regions of flanking native DNA (trnI F probe, GGCTATTAGCTCAGTGGTAGAGCGCGCCCCTGATAATTG, and trnI R probe, CCTGGCAAGTCTTTGTGAAATAACTCCG).

2.3.3. Gene expression analysis—Total RNA was isolated using Trizol (Invitrogen), further purified using an RNeasy column (Qiagen), and treated with DNase (Ambion). Reverse transcriptase (RT) primers were added to ~3–4 μg DNAse-treated RNA. RT primers (2.5 μM), targeted to junctions of genes within the insert, were, MVK end R, ACAGT-CATTAAAACTCCTCGTCTGAAGTCCATGG; AACT end R, GATATGAAACAGGAGGTATAACAATGAAACTCTC; HMGRt end R, GACTAGGC-CAGGATCGCTCTAGATGCATGC. SuperScript III First-Strand Synthesis System for RT-PCR was used (Invitrogen). The resulting cDNA was amplified using those and additional primers targeted to internal sequences as follows for the products indicated in Fig. 1: for product 1, PMK-F, TACAGCCTCGTCATCGGTGCCTTTAC, and PMK-R, GGTCTGGCAATCATCCAATAAGCTAGTTTGTAC; for product 2, MVK-F, GTGTGTCTGCGTTGAGAACCTACCTGC, and MVK-R, TACAGCCTCGTCATCGGTGCCTTTAC; for product 3, MDD-F, GGACGCCTCATTGCCCACATTATC, and MDD-R, CTTGTCCCATCCAGGAACA-GAGCCAAAC; for product 4, AACT-F, TGGTTCATTCCAGGGTTCTC-TATCCTCC, and AACT-R, CTCGTCCTTCGTGACTTGAGTATCAGGC; for product 5, HMGS-F, GATGGCGTTTCTCAAGGTAAATACACAATTG, and HMGS-R, TTGGGCAACTCTCTCTTTGTGGAATGGC; for product 6, HMGRt-F, CGTGGCTGTAAGGCAATCAATGCTG, and HMG Rt-R, GCAATGTTCAACTCAACCAATGCGG. All PCR products were sequenced to confirm identity.

2.4. Analysis of sterol and triglycerides

To analyze sterols and TAGs, fresh leaves of tobacco (100 g) were dried to constant weight at 95–100 °C using method 934.01 (AOAC 2000). The lipid measurements study was conducted in transplastomic plants when they were flowering. Lipids were extracted from dry samples with hexane and isopropanol (3:2) using a Dionex ASE 200 extractor (Dionex Corp.) as described (Schafer, 1998). One gram of each dry leaf sample was mixed with sand in a 20 mL extraction cell. Extraction conditions were the following: temperature 60 °C, pressure 2175 PSI, preheat 1 min, heat 5 min, static 10 min, flush 60 volume, purge 120 sec, cycle 2. Extracted lipid was transferred to a pre-weighed vial and dried under nitrogen in a 60°C bath. After the dry weight of the lipid fraction was determined, it was dissolved in 10 mL chloroform and methanol (5:2). A dissolved lipid sample (0.55 mL) was mixed with 2.2 mL of 1% (v/v) Triton-100 in chloroform (Carlson and Goldfarb, 1977) and evaporated to dryness at 37 °C under nitrogen. The sample was completely dissolved in deionized distilled water (1 mL) at 37 °C for 20 min. Total neutral sterols were analyzed in triplicate (Reagent kit 439–17501, Wako Diagnostics). Total TAGs were measured in triplicate (Reagent kit TR-22421, Thermo Clinical Chemistry). Values for sterols and TAGs were determined using several concentrations of the calibrators provided with the respective reagent kits.

2.5. Pigment extraction and analysis

Chlorophyll measurements were carried out using UV-vis spectroscopy as described (Lichtenthaler and Buschmann, 2001) on green leaf tissue (0.025 g) from 1-month old plants grown either in the greenhouse or in tissue culture. To extract carotenoids from tobacco, fully-expanded leaves of wildtype and transplastomic plants grown at the same time in the greenhouse from seed were freeze-dried by lyophilization. The dried leaves (2 g of each sample) were mixed in 10 mL ice-cold methylene chloride; 5 mL of each sample free from debris were retained. To separate carotenoids from chlorophylls, plant extracts were passed through a chromatography column, which contained 10 g of Alumina in 10 mL of hexane (Buckle and Rahman, 1979). Nine mL of hexane was used to elute carotenoids; eluate was divided into three samples. All preparations were carried-out on ice under darkened conditions. Samples were dried under a gentle stream of oxygen-free nitrogen gas and reconstituted in diethyl ether and ethyl acetate (1:1, v/v) for HPLC analysis.

Separation of carotenoids was performed using an Agilent 1200 Series HPLC system, with a 3 pm, 250 mm × 2.1 mm reverse phase Inertsil ODS-3 column (GL Sciences) at a flow rate of 0.4 ml min^{-1}. A sample injection volume of 2 μL was used throughout. The temperature of the sample tray was maintained at 4 °C by an Agilent FC/ALS Thermostat and the column at 32 °C. Peak responses (with an attenuation of 1000 mAU and a zero offset of 50 mAU) were determined using a diode array detector set at 460 nm. Compounds were identified by co-chromatography with standards (ß-carotene and lycopene in 50% diethyl ether/50% ethyl acetate; Sigma-Aldrich) and by elucidation of their spectral characteristics using a photo-diode array detector. β-carotene and lycopene were eluted with a linear gradient of ethyl acetate and 90% acetonitrile/10% water (100–60% from 0–13.74 min, 60–40% from 13.74–17.37 min, 40–0% from 17.37–17.44 min, 0–0% from 17.44–24.31 min, 0–100% from 24.31–24.38 min, and 100–100% from 24.38–34.00 min). Data acquisition and analysis were performed via the MassHunter software package (Agilent Technologies).

β-carotene and lycopene from plant extracts were quantified via five-point calibration curves ranging from 6.25 μM to 100 μM. The R^2 coefficient for β-carotene and lycopene calibration curves were 0.9976 and 0.9981, respectively. Individual carotenoid concentrations were calculated by comparing their relative proportions, as reflected by integrated HPLC peak areas, to total carotenoid content determined by spectrophotometry. The commercially obtained carotenoid standards were also subjected to the preparation protocol described above to determine the percentage recoveries. See Fig. S2a–f for analytical data.

2.6. Analysis of squalene

Squalene was extracted in the same way as carotenoids. The separation of squalene was conducted on a Cyclosil-B capillary column (30 m length, 0.25 mm internal diameter, and 0.25 mm film thickness; Agilent J & W Scientific) using an Agilent Technologies 6890 Series Gas Chromatograph (GC) system. The GC system was coupled to a Leap Technologies COMBI PAL (CTC Analytics) auto-sampler. A sample injection volume of 1 μL was used throughout, and the sample was injected in the splitless mode. Helium was used as the carrier gas at a constant flow rate of 36.6 mL/min. For the GC temperature gradient program, an initial isothermal heating of 210 °C was applied for 1 min; the temperature was then increased to 250 °C, at a rate of 3 °C min^{-1}, and held at 250 °C for a further 26 min.

The Agilent Technologies 6890 Series GC system was coupled to an Agilent 5973 Network Mass Selective Detector. The temperature of the inlet, transfer interface, and ion source was set to 250, 250, and 230 °C, respectively. A solvent delay of 3.5 min was implemented throughout the course of the experiment. Electron impact ionization (70 eV) was used and an acquisition rate of 0.98 cycles/s was employed. The fragment ions used for selected ion monitoring experiments were 69, 81, 95, and 410 *m/z* (the parent ion). The identification of squalene was based on the retention time, the abundance of the aforementioned fragment ions, and by standard addition. The fragment ion at 69 *m/z* was used for quantification as it is the most abundant ion in the mass spectrum of squalene. Data acquisition and analysis were performed via the Chemstation software package (Agilent Technologies). Squalene from the plant extract was quantified via a six-point calibration curve ranging from 62.5 nM to 200 μM. The R^2 coefficient for the calibration curve was 0.9987. See Fig. S3a–c for analytical data.

2.7. Analysis of mevalonate

The freeze-dried samples of wildtype and transplastomic leaves were used for separation of isoprenoid compounds (Frébortová et al., 2007). Before use, 5000-Da 4 mL filter units (Amicon Ultra, Millipore) were washed with 1 mL sterile water by centrifuging at 4000g for 2 h at 30 °C to remove glycerol and sodium salts. Leaf tissues (1.0 g) were ground in liquid nitrogen. Five mL 100% methanol (kept on dry ice) was added directly to the ground tissue and vigorously mixed, before centrifugation at 5000g at − 10 °C for 15 min. Supernatants were transferred to the washed filter units and centrifuged for 8 h at 4000g at − 10 °C to separate isoprenoid contents. All samples were kept on dry ice during the extraction procedure or stored at − 80 °C. Mevalonate was identified by retention time and accurate mass measurements.

The chemical standard for mevalonate was prepared by treating mevalonolactone (Sigma-Aldrich) with 2 M potassium hydroxide (Martin et al., 2003). The separation of the mevalonate was conducted on a ZIC-HILIC column (150 mm length, 2.1 mm internal diameter, and 3.5 μm particle size; from Merck SeQuant, and distributed via The Nest Group, Inc.) using an Agilent Technologies 1200 Series HPLC system (Agilent Technologies). The injection volume for the chemical standard and the metabolite was 2 μL. The temperature of the sample tray was maintained at 4 °C by an Agilent FC/ALS Thermostat. The column compartment was set to 32 °C. FPP was eluted isocratically with a mobile phase composition of 36% of 50 mM ammonium acetate, in water, and 64% of acetonitrile. A flow rate of 0.15 mL/min was used throughout. The HPLC system was coupled to an Agilent Technologies 6210 time-of-flight mass spectrometer (LC-TOF MS), by a 1/6 post-column split. Contact between both instruments was established by a LAN card in order to trigger the MS into operation upon the initiation of a run cycle from the MassHunter workstation (Agilent Technologies). Electrospray ionization (ESI) was conducted in the negative ion mode and a capillary voltage of − 3500 V was utilized. MS experiments were carried out in full scan mode, at 0.85 spectra/second and a cycle time of 1.176 s, for the detection of $[M-H]^-$ ions. The instrument was tuned for a range of 50–1700 *m/z*. Before analysis, the TOF MS was calibrated via an ESI-L-low concentration tuning mix (Agilent Technologies). Data acquisition and processing were performed by the MassHunter software package. Mevalonate from plant extracts was quantified via a seven-point calibration curve ranging from 625 nM to 50 μM. The R^2 coefficient for the calibration curve was 0.999.

2.8. Transmission electron microscopy

Leaf tissue (2 mm^2) from transplastomic and wildtype plants were fixed in 2.5% glutaraldehyde and 2% formaldehyde in 0.1 M sodium cacodylate buffer for several days. Fixed tissues were rinsed in the same buffer three times for 20–30 min per rinse and then post-fixed in 1% aqueous osmium tetroxide for 1 to 2 h. Samples were rinsed in water three times for 20–30 min and dehydrated in aqueous acetone (30%–50%–70%–95%–100%) three times for 30 min per step. Dehydrated samples were infiltrated and embedded in Spurr's resin. About 60 nm thick sections were collected on 400 mesh copper grids and stained in 2% uranyl acetate for 1 min, dried and viewed in the transmission electron microscope. Digital recordings were made on a Zeiss 902 electron microscope at 80 kV.

3. Results

3.1. Chloroplast transformation and functional expression of the cytoplasmic MEV pathway in chloroplasts

Targeting between *trnI* and *trnA* in the chloroplast genome sequence (Fig. 1a), the chloroplast transformation vectors pUY1 and pUYMEV6.1 (Fig. 1b–c) were used for genetic transformation of tobacco plants. The chloroplast transformation vectors contained the spectinomycin antibiotic resistant gene *aadA* (Svab and Maliga, 1993) as the first gene in the insert, located downstream from the 16S ribosomal RNA gene with its promoter. The pUY1 plasmid (derivative of pLDCtV; Guda et al., 2000) contains only the *aad*A gene and pUYMEV6.1 contains six genes encoding the six enzymes of the MEV pathway (Fig. S1).

Several independent transgenic shoots were recovered within 1–2 months from bombarded leaf tissue selected on RMOP medium supplemented with 500 mg/L spectinomycin. Transformed tissue was sub-cultured every two weeks on selection. Transplastomic plants containing the empty vector pUY1 or pUYMEV6.1 transferred to the greenhouse were routinely shorter than untransformed wildtype. Chloroplast transformation itself affected plant height. However, there were no differences in developmental phenotypes, including plant size, and shape and number of leaves, flowers and stems, between the original transplastomic lines. Also, transplastomic plants set seed normally. When we tested those seeds in tissue culture, they germinated normally and produced the same sized plants as untransformed wildtype seeds. Transplastomic lines grown in tissue culture did not exhibit developmental phenotypes, with or without the MEV pathway.

Integration of transgenes was confirmed by PCR using an internal primer that annealed to the coding region of *aad*A and one that annealed to the flanking sequence (Fig. 1b and c). In DNA from transplastomic plants the expected PCR products were amplified (Fig. 1d); 2.0 kb from pUY1 (T0-EV) and 10.0 kb from pUY-MEV6.1 tissue culture-derived plantlets #2, #3, and #4 (T0-mev). pUY-MEV6.1 T0 plant #4 and its seed-derived progeny (T1) appear to be homoplastomic, T0 #2 and T0 #3 heteroplastomic, and T0 #1 untransformed (Fig. 1d). Southern blots confirmed the site-specific integration of the expression cassette (Fig. 1e). Furthermore, we confirmed that pUY-MEV6.1 #4 is homoplastomic, as only one fragment hybridized with the probe in the T0 plantlet and T1 progeny (Fig. 1e). Transplastomic pUY-MEV6.1 T0 #2 and T0 #3 were confirmed to be heteroplastomic. To our knowledge, this report is the first describing integration of six foreign eukaryotic genes, plus a selectable marker gene into the chloroplast genome.

Transcription of the entire polycistronic insert engineered into tobacco chloroplasts was confirmed using reverse transcriptase (RT)-PCR on total RNA extracted from mature leaves. RNA was reverse transcribed using transgene junction-specific primers (Fig. 1f) and the cDNAs were then amplified with primers specific to the transgene sequences (Fig. 1g–i). All of the six MEV genes in the pUY-MEV6.1 #4 insert were expressed (Fig. 1j) indicating that the 16 S rRNA promoter functioned well to express the polycistronic message (seven genes including the selectable marker gene) from the pUY-MEV6.1 insert.

We used the response of transplastomic plantlets to growth on 100 μM fosmidomycin, which specifically inhibits the plastidial MEP pathway's enzyme, 1-deoxy-D-xylulose-5-phosphate reductoisomerase (DXR) (Zeidler et al., 1998), as a screen for the expression and functionality of the expressed protein products. Transplastomic seedlings (2 weeks old) of pUY1 T1 and pUY-MEV6.1 #4 T1 were transferred to fosmidomycin-supplemented medium for 2 weeks (Fig. 2). Transplastomic pUYMEV6.1 #4 T1 plants thrived on the fosmidomycin-supplemented medium (Fig. 2b). On the other hand, the transplastomic pUY1 T1 controls were three times smaller in size and bleached (Fig. 2a). The fact that the growth phenotype and pigmentation of the transplastomic T1 #4 seedlings were normal, compared to controls after growth on fosmidomycin-supplemented medium, indicates that the inhibition of the MEP pathway in pUY-MEV6.1 plants was complemented by the expression in the chloroplast of the introduced genes encoding the enzymes in the MEV pathway. Growth on 100 μM fosmidomycin was not lethal for the pUY1 transplastomic plants,

indicating that either there was residual MEP pathway expression or the cytosolic pathway provided necessary precursors.

We next analyzed levels of the intermediate metabolite mevalonate in leaves of transplastomic and control plants using a highperformance liquid chromatography time-of-flight mass spectrometer (HPLC-TOF-MS)-based metabolomics platform. Mevalonate accumulated in leaves of MEV6-containing transplastomic plants (mean ± SE=49 μmoles/g ± 13.3, n=3), but it was not detectable in the empty vector control or wildtype leaves. Increased levels of this intermediate indicate functionality of MEV6 transgene products to the point of production of mevalonate.

3.2. Impact on metabolism of expression of MEV pathway in chloroplasts

The MEP pathway produces chlorophylls and carotenoids (Lichthentaler, 2007). Levels of chlorophyll, ß-carotene, xanthophyll, and lycopene were analyzed. There was 1.4 times more ß-carotene in the MEV6 plants, when compared to empty vector controls (Fig. 3a). Lycopene and chlorophyll levels were not different in the transplastomic MEV6 and empty vector control plants and we were unable to detect xanthophylls.

To understand if cellular metabolism was affected by introducing the MEV biosynthetic pathway in tobacco chloroplasts, we measured levels of sterols, triacylglycerides (TAGs), and squalene in transplastomic plants. TAGs and sterols were measured at the flowering stage in T0 plants. The mean level of TAGs was slightly greater by 1.2 times in the MEV6-containing plants than the empty vector control (Fig. 3b). We observed that mean sterol levels in the MEV6-containing plants were twice those in the empty vector control plants (Fig. 3b). In addition, squalene was quantified in T1 plants at the 5-week vegetative stage. Squalene levels were 10 times higher in the MEV6-containing plants than in the empty vector controls (Fig. 3c). These results indicate that expression of the MEV pathway in chloroplasts enhances the levels of products associated with fatty acid synthesis and also, the cytoplasmic MEV pathway.

3.3. Effect on cellular structure

To assess the effect of the expression of the MEV6 pathway in chloroplasts at the cellular level, we examined leaf cells from transplastomic T1 lines by Transmission Electron Microscopy (TEM). TEM images of MEV6 samples were visually compared to those from the empty vector control (greenhouse grown plants 30- or 60-days old) in about 100 images each. Both mitochondria and chloroplasts were abundant and located in the peripherally located cytoplasm in mature mesophyll cells of the lines (Fig. 4). Chloroplast structure was not obviously affected by expressing the cytoplasmic MEV pathway; the size, shape, and prevalence of grana stacks, starch grains, and plastoglobuli were similar. Mitochondria were equally present in both lines.

There were two distinct differences in the ultrastructure of cells in the MEV6-containing transplastomic line. First, microbodies were located adjacent, and often appressed, to chloroplasts in the parietal cytoplasm in the MEV6 cells much more often than in the empty vector control sections (Fig. 4). Based on their appearance and size, many of these microbodies appeared to be peroxisomes (Gruber et al., 1970; Nishimura et al., 1993). The

peroxisomal matrix was granular and in many cases contained paracrystalline structures (Fig. 4c–d). On average, the paracrystalline structures filled less than one-fourth of the interior space. Second, there were oval to round bodies, with an electron translucent matrix containing an oval to round-shaped core of electron opaque material (Fig. 4e–g). These unidentified microbodies (UMB) were smaller than peroxisomes and some appeared to have a bilayer. UMB were absent in sections from the empty vector controls.

4. Discussion

Our results demonstrate that expression of the MEV6 pathway in the chloroplast resulted in an enhanced content of mevalonate and carotenoids. This suggests that increasing the availability of the IPP monomer resulted in enhanced flux through the downstream carotenoid biosynthetic pathway or enhanced expression or activity of the pathway. The complex regulation of carotenoid biosynthesis (Bouvier et al., 2005; Botella-Pavia et al., 2004; Fraser et al., 2009) suggests that many factors may impact levels. Although the genes encoding the MEV pathway to the point of production of IPP were added in our chloroplast manipulations, plastidal IPP isomerase expression was not manipulated. Tritsch et al. (2010) demonstrated that IPP isomerase acts to dynamically adjust the IPP/DMAPP ratio. It is possible that altering plastidal IPP isomerase expression would allow optimization of the ratio of IPP and DMAPP to further increase product levels (Martin et al., 2003).

Expression of the MEV pathway in chloroplasts enhanced the levels of products associated with fatty acid synthesis and, also, the cytoplasmic MEV pathway. Most fatty acids (16- and 18-carbon fatty acids) are synthesized from acetyl CoA in chloroplasts. Part of the fatty acid pool that is exported to the cytoplasm is assembled into storage lipids at the endoplasmic reticulum (ER), by donating fatty acyl groups to glycerol-3-phosphate to form TAGs. Under some developmental or stress conditions, chloroplasts synthesize TAGs as well (e.g., Kaup et al., 2002). The increase of fatty acid synthesis in response to expression of the MEV pathway in chloroplasts, as evidenced by an increased level of TAGs, indicates that acetyl CoA was freely available in the chloroplast and not limiting. It was shown earlier that acetyl CoA was not limiting with *p*-hydroxy-benzoic acid (pHBA) polymer accumulation (up to 26% dry weight) upon expression of chorismate pyruvte lyase in chloroplasts (Viitanen et al., 2004). Also, fatty acid synthesis was not adversely affected by production of polyhydroxybutyrate (PHB) in plastids, indicating that acetyl CoA was available (Poirier, 2002). However, the higher the accumulation of PHB, the more chlorosis and negative effects on plant growth were observed (Poirier, 2002). The direct expression of PHB synthesis in chloroplasts via integration of genes into the genome did not result in high levels of PHB and was also associated with chlorosis and negative effects on growth (Lossl et al., 2003). Although overexpression of MEV pathway enzymes is generally associated with alterations in the phenotype of plants, we did not detect developmental perturbations in our original MEV6 plants or tissue culture grown progeny thereof, when compared to empty vector controls.

Plant cells have delicately responsive mechanisms that sense levels of fatty acids and adjust metabolism to degrade or synthesize them, as needed (Eccleston and Ohlrogge, 1998). In leaves, excess fatty acids are degraded by β-oxidation in peroxisomes. Paradoxically, the

loss of fatty acids activates fatty acid synthesis in chloroplasts (Eccleston and Ohlrogge, 1998). The enhancement of TAG levels in the MEV6 transplastomic line reflects the result of an intriguing interplay between enhanced availability of isoprenoid substrates in the chloroplast, effects of isoprenoid intermediates on fatty acid synthesis (Kizer et al., 2008), and the balance of degradation of excess fatty acids in the cytosol with activation of fatty acid synthesis in the chloroplast. It seems possible that the increased numbers of peroxisomes and UMBs in the MEV6 transplastomic plants are caused by the need to eliminate excess fatty acids synthesized in response to the high and excess levels of substrates generated in the chloroplasts and exported to the cytosol or to increased TAG biosynthesis in the cytosol or chloroplast.

The additional, fully functioning pathway producing isoprenoid precursors in the chloroplast enhanced levels of squalene and sterols in transplastomic MEV6 plants. The enhanced levels most likely indicate that one or more metabolite exited the chloroplast and augmented the cytosolic pathway leading to their synthesis. This provides another example to the list of examples of cross talk between the two compartments (e.g., Gerber et al., 2009; Kasahara et al., 2002; Nagata et al., 2002). Labeling studies showed that the chloroplastidic MEP isoprenoid pathway contributes to biosynthesis of sterols (Arigoni et al., 1997; De-Eknamkul and Potduang, 2003) and volatile terpenes (Dudareva et al., 2005). IPP seemed to be transported from the chloroplast to the cytoplasm, but the plastidic transporter was not identified (Flügge and Gao, 2005). Mevalonate levels increased by expression of the mevalonate pathway in the chloroplast (Fig. 3) and studies in the future will ascertain if the mevalonate accumulated in the chloroplast or if it exited the chloroplast and accumulated in the cytosol. Whether mevalonate, IPP, or another metabolite, such as GPP or FPP is transported, the end result appears to be substrate movement across the chloroplast membrane, although we cannot formally rule out the possibility that the engineering of chloroplasts caused an induction of the cytosolic MEV pathway. It is possible that IPP or derived-metabolites only exit the chloroplast when concentrations exceed normal physiological levels, such as in our study. Our sterol results agree with earlier reports in which plant lines that over-expressed HMGR produced a few- to several-fold enhancement in total sterols (Schaller et al., 1995). In some cases, lipid bodies were observed in the cytoplasm of cells of tobacco (Gondet et al., 1994; Heyer et al., 2004). In all these examples, as in ours, there were no concomitant obvious morphological abnormalities. The interactions amoung levels of sterols, squalene, TAG, and expression of biosynthetic enzymes is complex (Wentzinger et al., 2002). Although squalene and TAG levels were enhanced, we observed that sterol levels were not enhanced to the same extent (Fig. 3). Wentzinger et al. (2002) also observed a concomitant accumulation of squalene and TAG. Squalene and TAG accumulated when sterol synthesis was inhibited in 3-day old tobacco cells in liquid culture treated for 2 h with a chemical inhibitor of squalene epoxidase. In light of this study and that squalene epoxidase should not have been limiting in our system, it is surprising that squalene accumulated to a greater extent than sterols. The fundamental differences in experimental systems may explain the discrepancy and would be of interest to study further. That our manipulations increased levels of isoprenoid intermediates suggests that our chloroplast-based strategy to increase levels of isoprenoid pathway precursors for valued cytosolic isoprenoids may with additional manipulations ultimately be successful. Applications may

include production of phytonutrients and phytopharmaceuticals, isoprenoid feedstocks for biofuels, and enhanced rubber production in rubber-producing plants.

We have no information, as yet on the true nature of composition of the UMB's observed in the MEV6 plants, but they are unlike other OsO_4-stained lipid bodies. However, in plants, isoprenoid pathway products are found in particles suspended in cytosol (latex), such as the granular electron-lucent particles in laticifers of the genus Papaver (Thureson-Klein, 1970) and rubber particles in rubber-producing plants (Rippel et al., 2003). Purified rubber particles have homogeneous, usually electron-dense cores, with a monolayer membrane (Cornish et al., 1999). Some rubber particles in *Parthenium argentatum* (guayule) cells, however, were without electron-opaque cores (Benedict et al., 2010).

Production of biopolymers in transgenic plants reached commercially viable levels with the accumulation of the pHBA polymer up to 26% dry weight in transplastomic plants (Viitanen et al., 2004). Unfortunately, high biopolymer accumulation in model plants generally negatively affects crop yield and other agronomic properties (Van Beilen and Poirier, 2008). Muntendam et al. (2009) assert that development of a microbial production platform for the biosynthesis of isoprenoids will offer cost-effective production, while eliminating climate and cultivation risks. However, the lack of an impact on plant development indicates that expression of the six additional MEV genes is not detrimental to chloroplast function and that diversion of acetyl CoA away from its normal distribution path in the chloroplast was not harmful. Thus, with sunlight fueling the entire process, production of isoprenoids via chloroplast engineering may overcome some of the limitations of a plant-based production platform. With clever engineering strategies, in which not only the precursor levels are elevated, but side reactions stifled (Kirby and Keasling, 2009), we predict additional improvements in production levels will lead to commercially-viable yields of desirable isoprenoid products.

Supplementary Material

Refer to Web version on PubMed Central for supplementary material.

Acknowledgments

We thank Darlene Hoffmann (San Joaquin Valley Agricultural Sciences Center, ARS, USDA, Parlier, California, USA) for performing TEM and Tina Williams (Western Regional Research Center, ARS, USDA, Albany, California, USA) for assisting in sample preparation for TEM. We thank Lewis Feldman, Steven Ruzin, Kent McDonald, Marisa Otegui, and Russell Jones for discussions of UMB. The authors received financial support from USDA ARS project 5325-41000-043-00D and Cooperative Research and Development Agreement #58-3K95-6-1172 with Yulex Corporation (Maricopa, Arizona).

Appendix A. Supplementary materials

Supplementary data associated with this article can be found in the online version at doi: 10.1016/j.ymben.2011.11.005.

Abbreviations

MEV mevalonate

MEP	2-C-methyl-D-erythritol 4-phosphate
IPP	isopentenyl diphosphate
DMAPP	dimethylallyl diphosphate
GPP	geranyl diphosphate
FPP	farnesyl diphosphate
GGPP	geranylgeranyl diphosphate
HMGR	3-hydroxy-3methylglutaryl-coenzyme A reductase
FPPS	FPP synthase
PTS	patchoulol synthase
DXS	1-deoxy-D-xylulose-5-phosphate synthase
DXR	1-deoxy-D-xylulose 5-phosphate reductoisomerase
PMK	phosphomevalonate kinase
MVK	mevalonate kinase
MDD	mevalonate diphosphate decarboxylase
AACT	acetoacetyl CoA thiolase
HMGS	HMGCoA synthase, acetoacetyl CoA thiolase
HMGRt	C-terminal truncated HMGCoA reductase
TAG	triacylglyceride
UMB	unidentified microbodies
ER	endoplasmic reticulum
pHBA	*p*-hydroxy-benzoic acid
PHB	polyhydroxybutyrate

References

Apel W, Bock R. Enhancement of carotenoid biosynthesis in trasplastomic tomatoes by induced lycopene-to-provitamin A conversion. Plant Physiol. 2009; 151:59–66. [PubMed: 19587100]

Arigoni D, Sagner S, Latzel C, Eisenreich W, Bacher A, Zenk MH. Terpenoid biosynthesis from 1-deoxy-D-xylulose in higher plants by intramolecular skeletal rearrangement. Proc Natl Acad Sci USA. 1997; 94:10600–10605. [PubMed: 9380681]

Bach TJ, Lichtenthaler HK. Inhibition by mevinolin of plant growth, sterol formation and pigment accumulation. Physiol Plant. 1983; 59:50–60.

Benedict CR, Gossa R, Greer PJ, Foster MA. The formation of rubber-producing cortical parenchyma cells in guayule (*Parthenium argentatum* Gray) by low temperature. Ind Crops Prod. 2010; 31:516–520.

Bick JA, Lange BM. Metabolic cross talk between cytosolic and plastidial pathways of isoprenoid biosynthesis: unidirectional transport of intermediates across the chloroplast envelope membrane. Arch Biochem Biophys. 2003; 415:146–154. [PubMed: 12831836]

Botella-Pavia P, Besumbes O, Phillips MA, Carretero-Paulet L, Boronat A, Rodriguez-Concepcion M. Regulation of carotenoid biosynthesis in plants: evidence for a key role of hydroxymethylbutenyl diphosphate reductase in controlling the supply of plastidial isoprenoid precursors. Plant J. 2004; 40:188–199. [PubMed: 15447646]

Bouvier F, Rahier A, Camara D. Biogenesis, molecular regulation and function of plant isoprenoids. Prog Lipid Res. 2005; 44:357–429. [PubMed: 16289312]

Buckle KA, Rahman FMM. Separation of chlorophyll and carotenoid pigments of capsicum cultivars. J Chromat A. 1979; 171:385–391.

Capell T, Christou P. Progress in plant metabolic engineering. Current Opinion Plant Bio. 2004; 15:148–154.

Carlson SE, Goldfarb S. A sensitive enzymatic method for the determination of free and esterified tissue cholesterol. Clin Chim Acta. 1977; 79:575–582. [PubMed: 890990]

Chappell J, VonLanken C, Vogeli U. Elicitor-inducible 3-hydroxy-3-methylglutaryl coenzyme A reductase activity is required for sesquiterpene accumulation in tobacco cell suspension cultures. Plant Physiol. 1991; 97:693–698. [PubMed: 16668454]

Cornish K, Wood DF, Windle JJ. Rubber particles from four different species, examined by transmission electron microscopy and electro-paramagnetic-resonance spin labeling, are found to consist of a homogenous rubber core enclosed by a contiguous, monolayer biomembrane. Planta. 1999; 210:85–96. [PubMed: 10592036]

Daniell H. Transgene containment by maternal inheritance: effective or elusive. Proc Natl Acad Sci USA. 2007; 104:6879–6880. [PubMed: 17440039]

Davidovich-Rikanati R, Lewinsohn E, Bar E, Iijima Y, Pichersky E, Sitrit Y. Overexpression of the lemon basil α-zingiberene synthase gene (ZIS) increases both mono- and sesquiterpene contents in tomato fruit. Plant J. 2008; 56:228–238. [PubMed: 18643974]

Davidovich-Rikanati R, Sitrit Y, Tadmor Y, Iijima Y, Bilenko N, Bar E, Carmona B, Fallik E, Dudai N, Simon JE, Pichersky R, Lewinsohn E. Enrichment of tomato flavor by diversion of the early plastidic terpenoid pathway. Nat Biotech. 2007; 25:899–901.

De-Eknamkul W, Potduang B. Biosynthesis of B-sitosterol and stigmasterol in *Croton sublyratus* proceeds via a mixed origin of isoprene units. Phytochemistry. 2003; 62:389–398. [PubMed: 12620352]

Dudareva N, Andersson S, Orlova I, Gatto N, Reichelt M, Rhodes D, Boland W, Gershenzon J. The nonmevalonate pathway supports both monoterpene and sesquiterpene formation in snapdragon flowers. Proc Natl Acad Sci USA. 2005; 102:933–938. [PubMed: 15630092]

Eccleston VS, Ohlrogge JB. Expression of lauroyl-acyl carrier protein thioesterase in *Brassica napus* seeds induces pathways for both fatty acid oxidation and biosynthesis and implies a set point for triacylglycerol accumulation. Plant Cell. 1998; 10:613–621. [PubMed: 9548986]

Enfissi EMA, Fraser PD, Lois LM, Boronat A, Schuch W, Bramley PM. Metabolic engineering of the mevalonate and non-mevalonate isopentenyl diphosphate-forming pathways for the production of health-promoting isoprenoids in tomato. Plant Biotech J. 2005; 3:17–27.

Flügge UI, Gao W. Transport of isoprenoid intermediates across chloroplast envelope membranes. Plant Biol. 2005; 7:91–97. [PubMed: 15666208]

Fraser PD, Enfissi EMA, Bramley PM. Genetic engineering of carotenoid formation in tomato fruit and the potential application of systems and synthetic biology approaches. Arch Biochem Biophys. 2009; 482:196–204.

Frébortová J, Galuszka P, Werner T, Schmulling T, Frébort I. Functional expression and purification of cytokinin dehydrogenase from *Arabidopsis thaliana* (AtCKX2) in *Saccharomyces cerevisiae*. Biol Plantarum. 2007; 51:673–682.

Gerber E, Hemmerlin A, Hartmann M, Heintz D, Hartmann MA, Mutterer J, Rodríguez-Concepción M, Boronat A, Van Dorsselaer A, Rohmer M, Crowell DN, Bach TJ. The plastidial 2-C-methyl-D-erythritol 4-phosphate pathway provides the isoprenyl moiety for protein geranylgeranylation in tobacco BY-2 cells. Plant Cell. 2009; 21:285–300. [PubMed: 19136647]

Gondet L, Bronner R, Benveniste P. Regulation of sterol content in membranes by subcellular compartmentation of steryl-esters accumulating in a sterol-overproducing tobacco mutant. Plant Physiol. 1994; 105:509–518. [PubMed: 12232218]

Gruber PJ, Trelease RN, Becker WM, Newcomb EH. A correlative ultrastructural and enzymatic study of cotyledonary microbodies following germination of fat-storing seeds. Planta. 1970; 93:269–288. [PubMed: 24496764]

Guda C, Lee SB, Daniell H. Stable expression of biodegradable protein based polymer in tobacco chloroplasts. Plant Cell Rep. 2000; 19:257–262.

Hahn FM, Eubanks LM, Testa CA, Blagg BS, Baker JA, Poulter CD. 1-Deoxy-D-xylulose 5-phosphate synthase, the gene product of open reading frame (ORF) 2816 and ORF 2895 in *Rhodobacter capsulatus*. J Bacteriol. 2001; 183:1–11. [PubMed: 11114895]

Hammerlin A, Bach TJ. Effects of mevinolin on cell cycle progression and viability of tobacco BY-2 cells. Plant J. 1998; 14:64–74.

Harker M, Holmberg N, Clayton JC, Gibbard CL, Wallace AD, Rawlins S, Hellyer SA, Lanot A, Safford R. Enhancement of seed phytosterol levels by expression of an N-terminal *Hevea brasiliensis* (rubber tree) 3-hydroxy-3-methylglutaryl-CoA reductase. Plant Biotechnol J. 2003; 1:113–121. [PubMed: 17147748]

Hasunuma T, Miyazawa S, Yoshimura S, Shinzaki Y, Tomizawa K, Shindo K, Choi S, Misawa N, Miyake C. Biosynthesis of astaxanthin in tobacco leaves by transplastomic engineering. Plant J. 2008b; 55:857–868. [PubMed: 18494855]

Hasunuma T, Takeno S, Hayashi S, Sendai M, Bamba T, Yoshimura S, Tomizawa K, Fukusaki E, Miyake C. Overexpression of 1-deoxy-D-xylulose-5-phosphate reductoisomerase gene in chloroplast contributes to increment of isoprenoid production. J Biosci Bioeng. 2008a; 105:518–526. [PubMed: 18558344]

Heyer J, Parker B, Becker DW, Ruffino J, Fordye A, De Witt M, Bedard M, Grebenok R. Steroid profiles of transgenic tobacco expressing an Actinomyces 3-hydroxysteroid oxidase gene. Phytochem. 2004; 65:2967–2976.

Kasahara H, Hanada A, Kuzuyama T, Takagi M, Kamiya Y, Yamaguchi S. Contribution of the mevalonate and methylerythritol phosphate pathways to the biosynthesis of gibberellins in Arabidopsis. J Biol Chem. 2002; 277:45188–45194. [PubMed: 12228237]

Kaup MT, Froese CD, Thompson JE. A role for diacylglycerol acyltransferase during leaf senescence. Plant Physiol. 2002; 129:616–626. [PubMed: 12068106]

Kirby J, Keasling JD. Biosynthesis of plant isoprenoids: perspectives for microbial engineering. Annu Rev Plant Biol. 2009; 60:335–355. [PubMed: 19575586]

Kizer L, Pitera DJ, Pfleger BF, Keasling JD. Application of functional genomics to pathway optimization for increased isoprenoid production. Appl Environ Microbiol. 2008; 74:3229–3241. [PubMed: 18344344]

Krichevsky A, Meyers B, Vainstein A, Maliga P, Citovsky V. Autoluminescent plants. PlosOne. 2010; 5:e15461 1–6.

Kumar S, Daniell H. Engineering the chloroplast genome for hyperexpression of human therapeutic proteins and vaccine antigens in recombinant protein protocols. Methods Mol Biol. 2004; 267:365–383. [PubMed: 15269437]

Laule O, Fürholz A, Chang HS, Zhu T, Wang X, Heifetz PB, Gruissem W, Lange BM. Crosstalk between cytosolic and plastidial pathways of isoprenoid biosynthesis in *Arabidopsis thaliana*. Proc Natl Acad Sci USA. 2003; 100:6866–6871. [PubMed: 12748386]

Lichtenthaler, HK., Buschmann, C. Current protocols in food analytical chemistry (CPFA). John Wiley; New York: 2001. Chlorophylls and carotenoids – measurement and characterisation by UV-vis; p. F4.3.1-F4.3.8.

Lichthentaler HK. Biosynthesis, accumulation and emission of carotenoids, alpha-tocopherol, plastoquinone, and isoprene in leaves under high photosynthetic irradiance. Photosynth Res. 2007; 92:163–179. [PubMed: 17634750]

Lossl A, Eibl C, Harloff HJ, Jung C, Koop HU. Polyester synthesis in transplastomic tobacco (*Nicotiana tabacum* L.): significant contents of polyhydroxybutyrate are associated with growth reduction. Plant Cell Rep. 2003; 21:891–899. [PubMed: 12789507]

Maliga P. Towards plastid transformation in flowering plants. Trends Biotechnol. 1993; 11:101–107.

Mandel MA, Feldmann KA, Herrera-Estrella L, Rocha-Sosa M, Leon P. CLA1, a novel gene required for chloroplast development, is highly conserved in evolution. Plant J. 1996; 9:649–658. [PubMed: 8653115]

Martin VJJ, Pitera DJ, Withers ST, Newman JD, Keasling JD. Engineering a mevalonate pathway in *Escherichia coli* for production of terpenoids. Nat Biotech. 2003; 21:796–802.

Muntendam R, Melillo E, Ryden A, Kayser O. Perspectives and limits of engineering the isoprenoid metabolism in heterologous hosts. Appl Microbiol Biotech. 2009; 84:1003–1019.

Nagata N, Suzuki M, Yoshida S, Muranaka T. Mevalonic acid partially restores chloroplast and etioplast development in Arabidopsis lacking the non-mevalonate pathway. Planta. 2002; 216:345–350. [PubMed: 12447549]

Nishimura M, Takeuchi Y, De Bellis L, Nishimura H. Leaf peroxisomes are directly transformed to glyoxysomes during senescence of pumpkin cotyledons. Protoplasma. 1993; 175:131–137.

Oey M, Lohse M, Kreikemeyer B, Bock R. Exhaustion of the chloroplast protein synthesis capacity by massive expression of a highly stable protein antibiotic. Plant J. 2009; 57:436–445. [PubMed: 18939966]

Poirier Y. Polyhydroxyalakanote synthesis in plants as a tool for biotechnology and basic studies of lipid metabolism. Pro Lipid Res. 2002; 41:131–155.

Quesada-Vargas R, Ruiz ON, Daniell H. Characterization of heterologous multi-gene operons in transgenic chloroplasts: transcription, processing and translation. Plant Physiol. 2005; 138:1746–1762. [PubMed: 15980187]

Rippel MM, Lee LT, Leite C, Galembeck F. Skim and cream natural rubber particles: colloidal properties, coalescence and film formation. J Colloid Interface Sci. 2003; 268:330–340. [PubMed: 14643232]

Ruhlman T, Verma D, Samson N, Daniell H. Role of heterologous elements in transgene integration and expression. Plant Physiol. 2010; 152:2088–2104. [PubMed: 20130101]

Schafer K. Accelerated solvent extraction of lipids for determining the fatty acid composition of biological material. Anal Chim Acta. 1998; 358:69–77.

Schaller H, Grausem B, Benveniste P, Chye ML, Tan CT, Song YH, Chua NH. Expression of the Hevea brasiliensis (H.B.K.) Müll. Arg 3-hydroxy-3-methylglutaryl-coenzyme A reductase 1 in tobacco results in sterol over-production. Plant Physiol. 1995; 109:761–770. [PubMed: 12228630]

Steliopoulos P, Wust M, Adam KP, Mosandl A. Biosynthesis of the sesquiterpene germacrene D in *Solidago canadensis*: ^{13}C and ^{2}H labeling studies. Phytochemistry. 2002; 60:13–20. [PubMed: 11985846]

Suzuki M, Nakagawa S, Kamide Y, Kobayashi K, Ohyama K, Hashinokuchi H, Kiuchi R, Saito K, Muranaka T, Nagata N. Complete blockage of the mevalonate pathway results in male gametophyte lethality. J Exp Bot. 2009; 60:2055–2064. [PubMed: 19363204]

Svab Z, Maliga P. High-frequency plastid transformation in tobacco by selection for a chimeric aadA gene. Proc Natl Acad Sci USA. 1993; 90:913–917. [PubMed: 8381537]

Thureson-Klein A. Observations on the development and fine structure of the articulated laticifers of *Papaver somniferum*. Annals Bot. 1970; 34:751–759.

Tritsch D, Hemmerlin A, Bach TJ, Rohmer M. Plant isoprenoid biosynthesis via the MEP pathway: in vivo IPP/DMAPP ratio produced by (E)-4-hydroxy-3-methylbut-2-enyl diphosphate reductase in tobacco BY-2 cell cultures. FEBS Lett. 2010; 584:129–134. [PubMed: 19903472]

Van Beilen JB, Poirier Y. Production of renewable polymers from crop plants. Plant J. 2008; 54:684–701. [PubMed: 18476872]

Viitanen PV, Devine AL, Khan MS, Deuel DL, Van Dyk DE, Daniell H. Metabolic engineering of the chloroplast genome using the *Escherichia coli* ubiC gene reveals that chorismate is a readily abundant plant precursor for p-Hydroxybenzoic acid biosynthesis. Plant Physiol. 2004; 136:4048–4060. [PubMed: 15563620]

Wentzinger LF, Bach TJ, Hartmann MA. Inhibition of squalene synthase and squlene epoxidase in tobacco cell striggers an up-regulation of 3-hydroxy-3-methylglutaryl coenzyme A reductase. Plant Physiol. 2002; 130:334–346. [PubMed: 12226513]

Wu S, Schalk M, Clark A, Miles RB, Coates R, Chappell J. Redirection of cytosolic or plastidic isoprenoid precursors elevates terpene production in plants. Nat Biotechnol. 2006; 24:1441–1447. [PubMed: 17057703]

Zeidler J, Schwender J, Müller C, Wiesner J, Weidemeyer C, Back E, Jomaa H, Lichtenthaler HK. Inhibition of the non-mevalonate 1-deoxy-D-xylulose-5-phosphate pathway of plant isoprenoid biosynthesis by fosmidomycin. Z Naturforsch. 1998; 53:980–986.

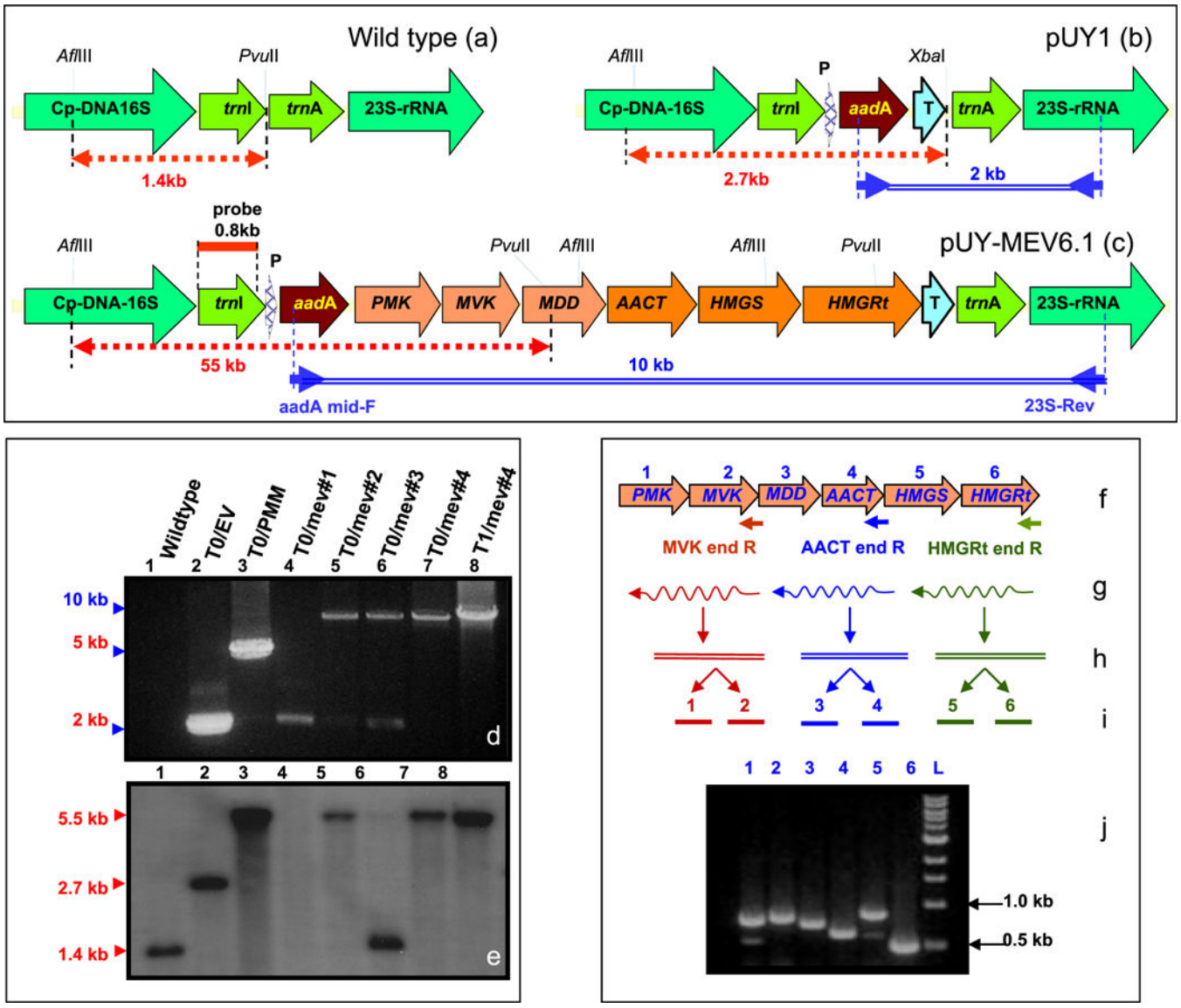

Fig. 1.

Transgene integration into chloroplast genome. Physical maps of tobacco chloroplast transformation target region in wildtype chloroplast genome (a) with intragenic region in between *trnI* and *trnA* as the integration site for transgenes; transplastomic genomic regions post-integration of (b) pUY1 vector, with promoter *Prrn* (P) driving expression of *aadA* for spectinomycin resistance, or (c) pUY-MEV6.1, containing six yeast genes encoding the cytoplasmic mevalonate pathway. Primer annealing sites (blue arrowheads) and PCR amplified products (blue line) post-integration shown in b and c; PCR products (d) amplified using primers aadA-mid-F (internal to construct) and 23 S-Rev (external to integrated construct) in transplastomic plants. Southern blot (e) probe (solid red line in c) and hybridizing DNA fragments (dashed red lines) in genomic DNA (2 mg) from wildtype and transplastomic T0 and T1 lines digested with *Afl*III and *Pvu*II (a), *Afl*III and *Xba*I (b), and *Afl*III and *Pvu*II (c). Homoplasmy is evident in T0- MEV6 #4 and its selfed progeny T1-MEV6 #4. Expression of mevalonate pathway genes inserted into tobacco chloroplasts (f–j).

Total RNA from (f) transplastomic T0 #4 was reverse transcribed (g) using junction-specific primers. Resulting cDNAs (h) were amplified with gene-specific primers and (i) PCR products were fractionated by electrophoresis (j), with numbers above the lanes referring to the numbers above the genes labeled in (f).

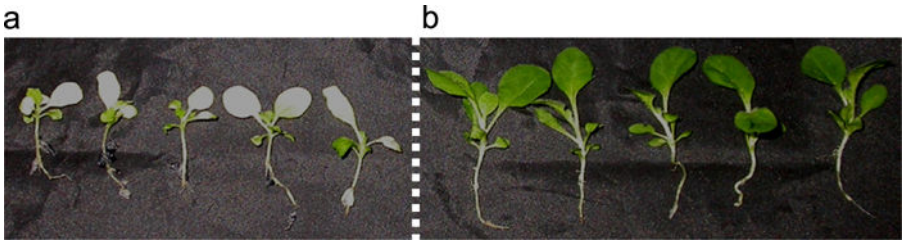

Fig. 2.

Phenotypic analysis of transplastomic lines. Complementation of fosmidomycin-induced inhibition of the chloroplastic MEP pathway by expression of the cytoplasmic mevalonate pathway of yeast in tobacco chloroplasts is shown, where seeds of transplastomic tobacco lines transformed with (a) pUY or (b) pUY-MEV6.1 were grown on RMOP medium containing spectinomycin for two weeks, then transferred to the same medium containing fosmidomycin (100 μM) for two additional weeks.

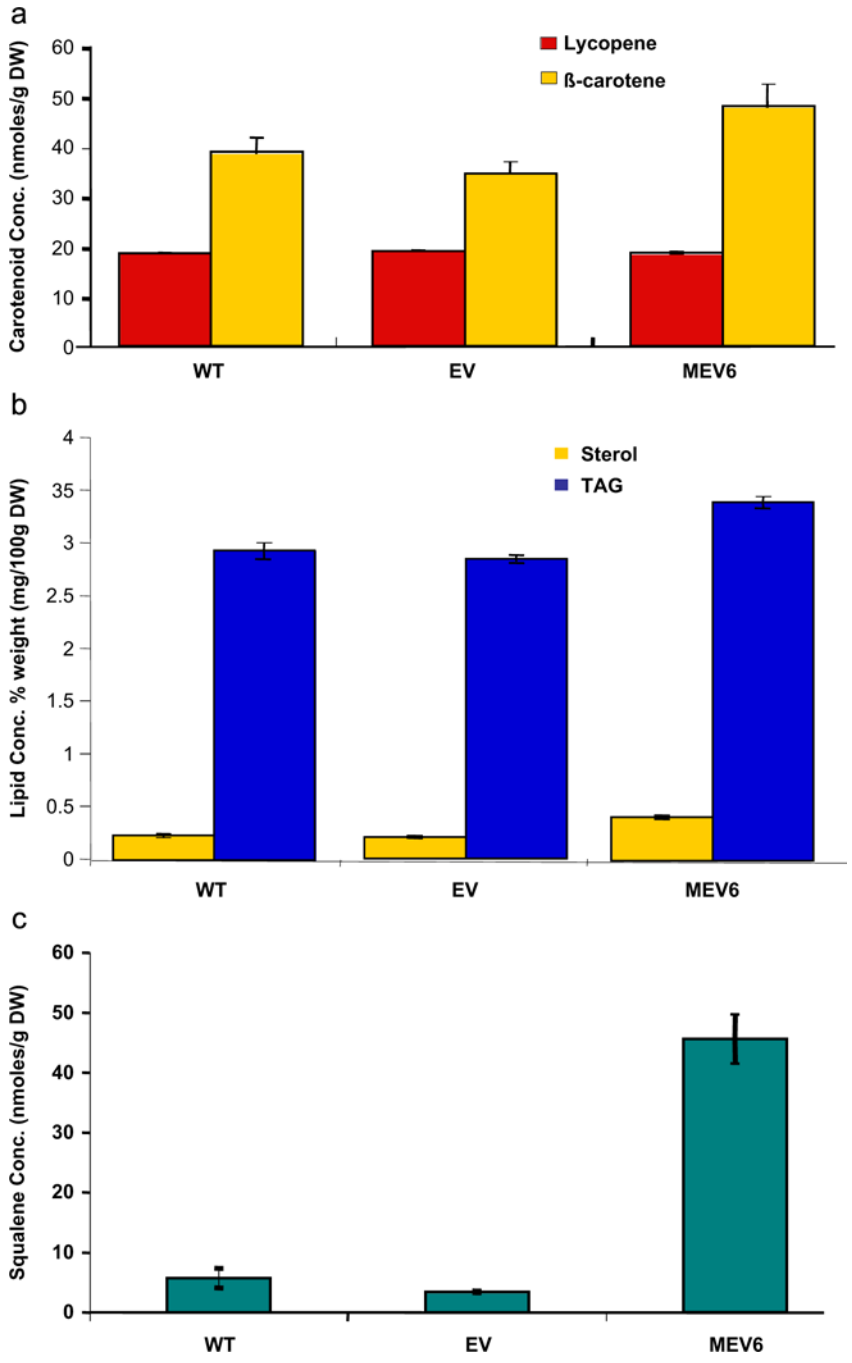

Fig. 3.

Impact of MEV6 pathway expression in chloroplast on isoprenoid metabolites. (a) Mean relative amounts of ß-carotene and lycopene ± SE (n=3) were measured by reverse phase HPLC from leaves of one month old plants. Peaks were identified on the basis of retention time and spectra compared with standards. (b) Mean percent dry weight of total lipids ± SE (n=3) that are sterols and triacylglycerides in mature leaves. (c) Mean squalene (μM) ± SE (n=3) quantified using GC−MS from seedling leaves.

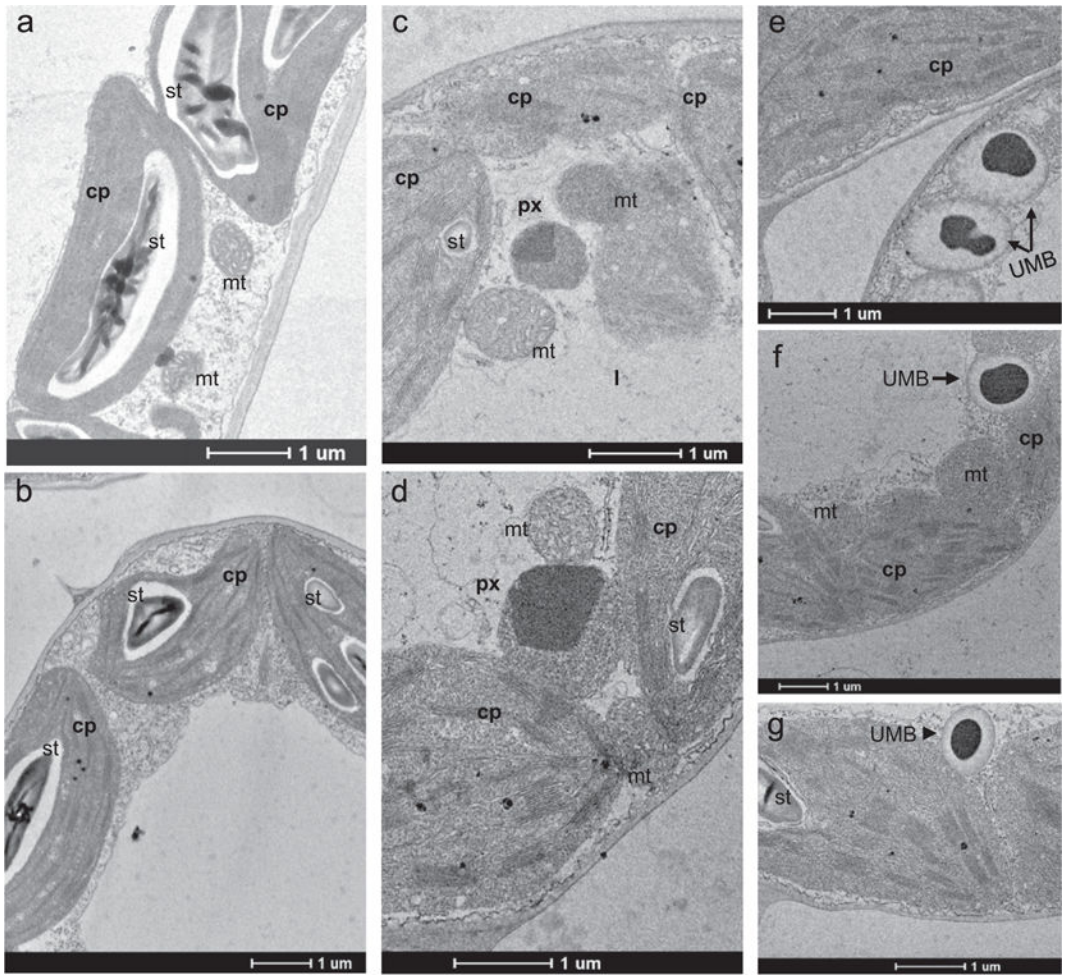

Fig. 4.

Electron micrographs of tobacco leaf mesophyll cells from (a) wildtype, (b) empty vector transplastomic control line, and (c–g) MEV6-containing transplastomic line. Leaves were isolated from 60 day-old plants grown in the greenhouse. Chloroplasts (cp) containing starch granules (st) and mitochondria (mt) are located in the parietal cytoplasm. In MEV6 transplastomic line sections, peroxisomes (px) are closely associated with chloroplasts and contain a paracrystalline structure (c–d). Unidentified microbodies (UMB) with electron dense cores were also observed in the MEV6 cells (e–g).